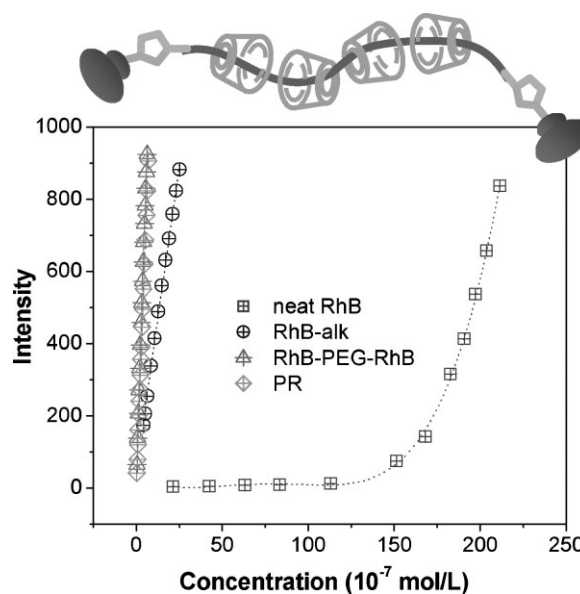


# Click Chemistry Approach to Rhodamine B-Capped Polyrotaxanes and their Unique Fluorescence Properties<sup>a</sup>

Jiayan Wu, Chao Gao\*

A fluorescent polyrotaxane (PR) made from the diazido-poly(ethylene glycol) (N<sub>3</sub>-PEG-N<sub>3</sub>) axis,  $\alpha$ -cyclodextrins, and alkyne-functionalized rhodamine B (RhB-alk) stoppers via Cu(I)-catalyzed azide–alkyne click chemistry is reported. A nanowire-like morphology of the prepared fluorescent PRs was visualized by atomic force microscopy. The fluorescence emission intensities of RhB-capped PEG (RhB-PEG-RhB) and the PR were much higher than that of neat RhB or RhB-alk with the same concentration of RhB fluorophore in both dimethylsulfoxide and alkaline aqueous solutions. Fluorescence lifetimes were detected as 3.59, 3.31, 2.99, and 2.99 ns for neat RhB, RhB-alk, RhB-PEG-RhB, and the PR, respectively. The PRs with unique fluorescence properties might have further applications in the fields of biomedicine and bionanotechnology.



## Introduction

Since the discovery of polyrotaxane (PR) and pseudo-PR consisting of cyclodextrins (CDs) and poly(ethylene glycol) (PEG) by Harada et al.<sup>[1]</sup> in the 1990s, various fruits have been harvested in the synthesis of PRs with different terminal bulky stoppers.<sup>[2]</sup> These efforts not only enriched the structures of PRs, but also demonstrated the promising applications of PRs in the fields of slide-ring materials,<sup>[3]</sup> efficient drug delivery systems,<sup>[4]</sup> molecular tubes,<sup>[5]</sup> and so forth.<sup>[6]</sup>

Many different preparation methods for PRs based on PEG and CDs have been developed nowadays in terms of end-capping reactions: for instance, 1) end-capping of diamino-PEG with 2,4-dinitrofluorobenzene to form an amine linkage;<sup>[7]</sup> 2) end-capping of diamino-PEG with L-Phe succinimide to form a biodegradable peptide linkage;<sup>[8]</sup> 3)

J. Wu, C. Gao

Key Laboratory of Macromolecular Synthesis and Functionalization (Ministry of Education), Department of Polymer Science and Engineering, Zhejiang University, 38 Zheda Road, Hangzhou 310027, P. R. China  
E-mail: chaogao@zju.edu.cn

J. Wu

College of Chemistry and Chemical Engineering, Shanghai Jiao Tong University, 800 Dongchuan Road, Shanghai 200240, P. R. China

<sup>a</sup> Supporting information for this article is available at the bottom of the article's abstract page, which can be accessed from the journal's homepage at <http://www.mcp-journal.de>, or from the author.

end-capping of dihydroxy-PEG (HO-PEG-OH) with isocyanate derivative of the fluorescent molecule to form a carbamate linkage;<sup>[9]</sup> 4) end-capping of diamino-PEG with sulfonyl chloride to form a sulfonamide linkage;<sup>[10]</sup> 5) end-capping of dicarboxylic-PEG with adamantamine to form an ester linkage;<sup>[11]</sup> 6) end-capping of diamino-disulfide-PEG with benzyloxycarbonyl tyrosine to form a biodegradable disulfide linkage;<sup>[12]</sup> 7) photodimerization of the 2-anthryl groups at the ends of PEG axis.<sup>[13]</sup> In addition to the synthesis methods mentioned above, various research groups also did some further works in the synthesis, modification, and application of the PRs.<sup>[3,14–26]</sup>

Due to the strong hydrogen bonds between CDs and water molecules, it is very hard to remove the residual water from the pseudo-PRs completely. So the ideal end-capping reaction should be tolerant of water and also fast enough to keep CD beads threading on the axis as many as possible, to obtain the PR with high threading efficiency. “Click” chemistry, the Huisgen 1,3-dipolar cycloaddition of azides and alkynes, was chosen as the end-capping reaction here. The click reaction has been widely demonstrated as a convenient technique in the design and synthesis of multifunctional molecules and materials for its intrinsic advantages, such as, modular, wide in scope, giving very high yields, no byproducts, tolerance of water, and so on.<sup>[27–40]</sup> Click reaction has been used by many investigators in the synthesis of rotaxanes.<sup>[41]</sup> However, few scientists have ever employed click coupling in the end-capping reactions of PRs since the first successful try was reported.<sup>[42]</sup>

This article aims to provide a click chemistry-based methodology to prepare the PRs with fluorescent stoppers which are suitable to work as drug carriers and other self-detectable frameworks. Accordingly, we design a molecular model of the target PRs, as shown in Figure 1. Herein, rhodamine B (RhB) is selected as the fluorescent stopper which is widely used in the bioimaging because of its high fluorescence quantum yield.<sup>[43]</sup> Ester bonds are introduced to both ends of the PEG axis, which can hydrolyze to release  $\alpha$ -CDs and their derivatives if required. In addition, the size of the PRs should be taken into consideration as well,

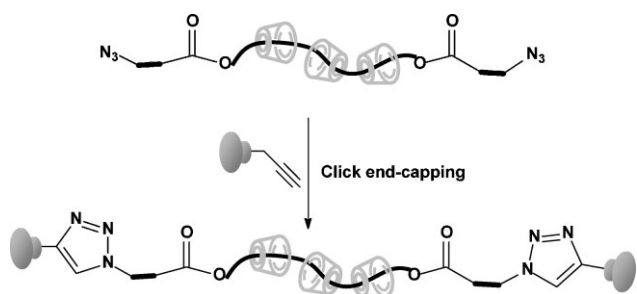


**Figure 1.** Molecule design for PR possessing ester groups and fluorescent RhB stoppers via click end-capping reaction.

because of the limitation of molecular size for the biological application. We found, according to ref. [12], the PRs consisting of PEG with number-average molecular weight ( $\bar{M}_n$ ) of 4 000, successfully worked as efficient gene carriers. So among the commercially available HO-PEG-OH, the HO-PEG-OH with  $\bar{M}_n$  of 4 600 is suitable to work as the axis of our designed biocompatible PR. After the pseudo-PRs possessing azido groups at both ends of PEG axes are prepared, the PRs can be accessed by azide–alkyne click coupling with alkyne-functionalized RhB (RhB-alk). Significantly, we not only got the fluorescent PRs successfully, but also found unique fluorescence properties of the PRs indeed and observed the nanostructures of the PRs with atomic force microscopy (AFM).

## Experimental Part

### Materials

4-(Dimethylamino) pyridine (DMAP, 99%), sodium azide (99%), succinic anhydride (98%), propargyl alcohol (99%), and 1,1,4,7,7-pentamethyldiethylenetriamine (PMDETA, 98%) were all purchased from Alfa Aesar. *N,N*-Dicyclohexylcarbodiimide (DCC, 98%), *N*-(3-dimethylaminopropyl)-*N'*-ethylcarbodiimide hydrochloride (EDC·HCl, 99%), and *N*-hydroxysuccinimide (NHS, 98%) were obtained from GL Biochem Shanghai Ltd. HO-PEG-OH ( $\bar{M}_n = 4 600$ , 98%), RhB (95%), valeryl chloride (98%), and CuBr (purified according to ref. [34] before use, 98%) were purchased from Sigma–Aldrich.  $\alpha$ -CD (99%) was the product of Shaanxi Liquan Chemical Co., Ltd. Dimethylsulfoxide (DMSO) and all the other solvents were purchased from Sinopharm Chemical Reagent Co., Ltd. Triethylamine (TEA) and dichloromethane were dried with  $\text{CaH}_2$  and distilled under reduced pressure before use. *N,N*-Dimethylacetamide (DMAC) and dimethylformamide (DMF) were dried with  $\text{MgSO}_4$  overnight prior to use. 2-Azidoethanol and 4-(2-azidoethoxy)-4-oxobutanoic acid (carboxylic azide) were synthesized in our laboratory according to the previous procedures.<sup>[44]</sup>

### Characterization

Ultraviolet (UV–Vis) spectra, fluorescence emission spectra, and gel permeation chromatography (GPC) were recorded on a PerkinElmer Lambda 20/2.0 UV–Vis spectrometer, PerkinElmer LS 50B spectrometer (the emission slit was 5 nm), and PerkinElmer HP 1100 (LiBr/DMF 0.01 mol·L<sup>-1</sup> as the eluent, RI-WAT 150CV+ as a detector, and polystyrene as a standard at 70 °C), respectively. <sup>1</sup>H NMR (400 MHz) and <sup>13</sup>C NMR (100 MHz) measurements were carried out on a Varian Mercury plus 400 NMR spectrometer using  $\text{CDCl}_3$  and  $\text{DMSO}-d_6$  as solvents. Fourier transform infrared (FT-IR) spectra were recorded on a PE Paragon 1000 spectrometer (KBr disk and film). Wide-angle X-ray diffraction (WAXD) patterns were obtained by using Rigaku III Dmax 2500 diffractometer with Cu radiation 35 kV, 25 mA at 4.0°·min<sup>-1</sup>. AFM was performed on a NanoScope IIIa SPM from Digital instruments Inc. under tapping mode. The compound was dissolved in DMSO and then a drop of this solution applied onto a mica substrate. After the solvent was removed by

heating at 60 °C under vacuum, the sample was imaged by AFM. Fluorescence lifetimes were measured with Edinburgh instruments FLS 920. A flash lamp (nF900, 2.5 ns) was used to excite the samples and reconvolution fitting was utilized as the data analysis method with instrument respond function.

### Synthesis of Diazido-Poly(Ethylene Glycol) (N<sub>3</sub>-PEG-N<sub>3</sub>)

DCC (3.66 g, 17.39 mmol) was added to a 250 mL Schlenk flask containing 120 mL dried CH<sub>2</sub>Cl<sub>2</sub> under nitrogen and the reaction mixture was cooled in an ice bath. After DCC was dissolved, HO-PEG-OH (20.00 g, ca. 8.70 mmol –OH) and carboxylic azide (3.25 g, 17.39 mmol) were added to the flask subsequently under magnetic stirring. Then 216.0 mg (1.75 mmol) of DMAP dissolved in 3 mL dried CH<sub>2</sub>Cl<sub>2</sub> was added into the mixture within 10 min. The reaction mixture was allowed to react in the ice bath for 1 h and then at room temperature for 2 d. The reaction mixture was filtrated to remove the white precipitate and then washed subsequently with 1 M HCl aqueous solution (3 × 100 mL), 1 M NaOH aqueous solution (3 × 100 mL), and 1 M NaCl aqueous solution (3 × 100 mL). The organic layer was dried over anhydrous MgSO<sub>4</sub> overnight, and then purified by precipitating in ethyl ether twice. The precipitate was collected and dried under vacuum at 40 °C for 24 h to get a white powder. Yield: 14.22 g, 66%. <sup>1</sup>H NMR (CDCl<sub>3</sub>, δ, ppm): 4.22 (m, 8H, N<sub>3</sub>CH<sub>2</sub>CH<sub>2</sub>O and COOCH<sub>2</sub>CH<sub>2</sub>O), 3.61 (s, N<sub>3</sub>CH<sub>2</sub>CH<sub>2</sub>O and CH<sub>2</sub> of PEG), 2.68 (s, 8H, OCOCH<sub>2</sub>CH<sub>2</sub>COO). <sup>13</sup>C NMR (CDCl<sub>3</sub>, δ, ppm): 171.12 (N<sub>3</sub>CH<sub>2</sub>CH<sub>2</sub>OCO), 170.91 (COOCH<sub>2</sub>CH<sub>2</sub>O), 69.56 (C of PEG), 68.03 (COOCH<sub>2</sub>CH<sub>2</sub>O), 62.92 (COOCH<sub>2</sub>CH<sub>2</sub>N<sub>3</sub>), 62.20 (COOCH<sub>2</sub>CH<sub>2</sub>O), 48.68 (COOCH<sub>2</sub>CH<sub>2</sub>N<sub>3</sub>), 27.91 (OCOCH<sub>2</sub>CH<sub>2</sub>COO). FT-IR (film, cm<sup>-1</sup>): 2 106 (N<sub>3</sub>), 1 738 (CO).

### Synthesis of Alkyne-Functionalized Rhodamine B

The synthesis route of RhB-alk was similar with that in ref.<sup>[45]</sup>. EDC · HCl (3.24 g, 16.7 mmol) was added to an anhydrous CH<sub>2</sub>Cl<sub>2</sub> solution of RhB (5.03 g, 10.5 mmol), followed by NHS (1.34 g, 11.5 mmol). After the reaction mixture was stirred for 1 h at room temperature under nitrogen, propargyl alcohol (2.37 g, 41.7 mmol) and DMAP (128.8 mg, 1.0 mmol) dissolved in 2 mL anhydrous CH<sub>2</sub>Cl<sub>2</sub> were added to the reaction mixture dropwise. The reaction mixture was stirred at room temperature for 2 d and then poured into ethyl ether to get the product. Yield: 3.81 g, 70%. <sup>1</sup>H NMR (CDCl<sub>3</sub>, δ, ppm): 1.22 (q, 12H, CH<sub>3</sub>), 2.44 (s, 1H, CH≡C), 3.66 (m, 8H, CH<sub>2</sub>N), 4.64 (s, 2H, OCH<sub>2</sub>C≡CH), 6.98–8.24 (m, 10 H, H of benzene ring).

### Synthesis of Pseudo-Polyrotaxane

The synthesis method of pseudo-PR was similar with that reported in ref. [7]. Under room temperature, a water solution containing 1.00 g (0.2 mmol) N<sub>3</sub>-PEG-N<sub>3</sub> was added into a saturated water solution of 10.00 g (10.3 mmol) α-CDs and then the mixture was stirred for 4 d. After filtering and washing with water several times to remove the unthreaded α-CDs, the precipitate was dried under vacuum at 65 °C for 2 d to get a white powder. Yield: 6.3 g, 57%.

### Synthesis of Fluorescent Polyrotaxane

Under room temperature, RhB-alk (0.50 g), CuBr (83.2 mg, 0.6 mmol), pseudo-PR (0.50 g), and PMDETA (123 μL, 0.6 mmol) were added to 5 mL anhydrous DMF subsequently under nitrogen. The mixture was stirred under room temperature for 24 h and then poured into deionized water. The collected red precipitate was repeatedly washed with water and anhydrous alcohol until RhB-alk could not be detected by UV-Vis spectrometer in the concentrated washing solution. The precipitate was dried under vacuum at 50 °C for 24 h to get a red powder. Yield: 35.5 mg, 7%. <sup>1</sup>H NMR (DMSO-*d*<sub>6</sub>, δ, ppm): 6.90–7.08 (m, H of benzene rings), 5.40–5.53 (m, OH-2,3), 4.78 (m, H-1), 4.46 (m, OH-6), 3.53–3.81 (m overlapped, H-3,5,6), 3.49 (CH<sub>2</sub> of PEG), 3.37 (m, H-2), 3.28 (m, H-4), 1.20 (t, CH<sub>3</sub>).

### Synthesis of Valeryl Chloride-Modified Polyrotaxane

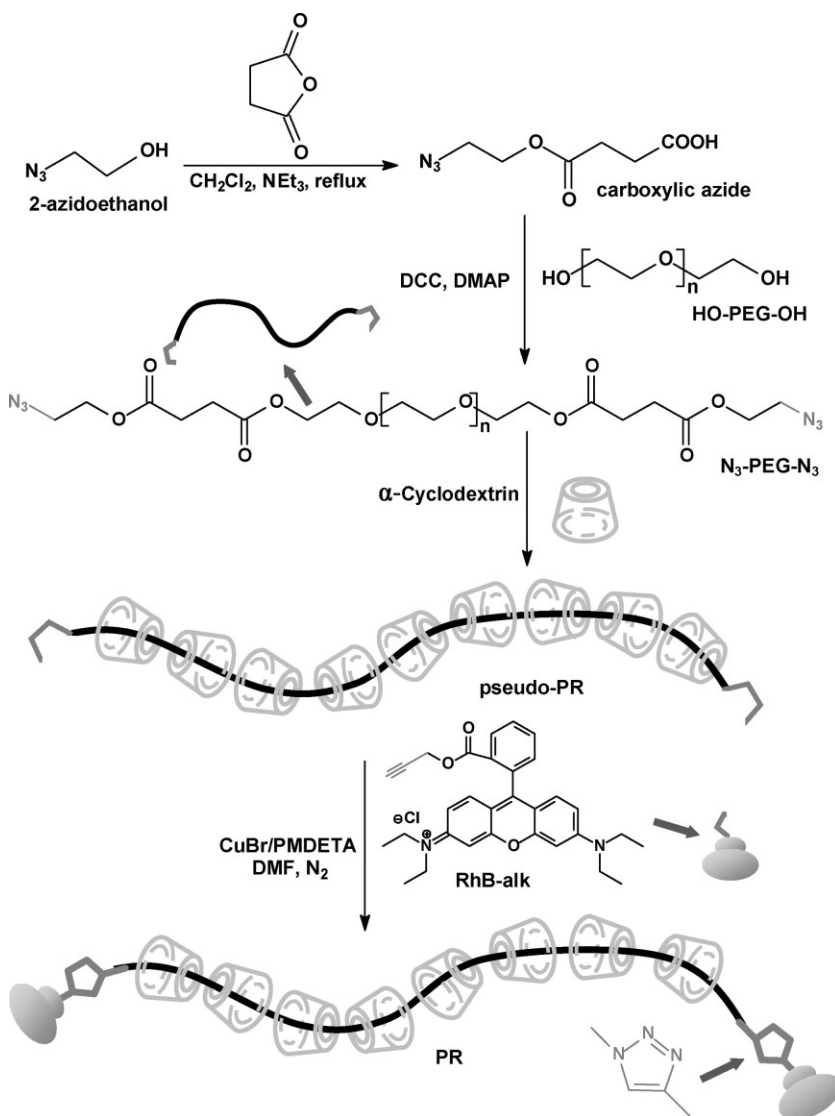
According to ref.<sup>[46]</sup>, 10.6 mg of PR (ca. 0.2 mmol OH groups) and 0.5 mL TEA were dissolved in 1 mL of dry DMAc containing 8% w/w lithium chloride (LiCl). To this solution, valeryl chloride (45.1 mg, 0.4 mmol, ca. 2.0 equiv. to the OH groups of the PR) dissolved in dry DMAc (0.5 mL) was added slowly under nitrogen at 0 °C. After stirring under room temperature overnight, the reaction mixture was poured into ethanol. The precipitate was collected by centrifugation, washed with water several times, and dried under vacuum at 65 °C for 24 h to get a red powder. Yield: 9.6 mg, 35%,  $\bar{M}_n = 43\ 600$ ;  $\bar{M}_w/\bar{M}_n = 1.13$ . <sup>1</sup>H NMR (DMSO-*d*<sub>6</sub>, δ, ppm): 0.85 (t, 54 H, CH<sub>3</sub>), 1.27 (m, 36 H, CH<sub>2</sub>CH<sub>3</sub>), 1.50 (m, 36 H, CH<sub>2</sub>CH<sub>2</sub>CH<sub>3</sub>), 2.32 (m, 36 H, COCH<sub>2</sub>), 3.49 (CH<sub>2</sub> of PEG), 3.31–5.00 (m overlapped, 42 H, H of the PR) (see Figure S1 of Supporting Information).

### Synthesis of Rhodamine B-Capped Poly(Ethylene Glycol)

The synthesis route of RhB-PEG-RhB was quite similar with that of the PRs. Under room temperature, RhB-alk (0.50 g), CuBr (83.2 mg, 0.6 mmol), N<sub>3</sub>-PEG-N<sub>3</sub> (0.50 g), and PMDETA (123 μL, 0.6 mmol) were added subsequently to 5 mL anhydrous DMF under nitrogen. The mixture was stirred under room temperature for 24 h and then poured into ethyl ether. The precipitate was collected and redissolved in CH<sub>2</sub>Cl<sub>2</sub>. The solution was washed subsequently with 1 M NaOH aqueous solution (10 × 100 mL) and 1 M NaCl aqueous solution (5 × 100 mL). The organic layer was dried over anhydrous MgSO<sub>4</sub> overnight, and then poured into ethyl ether after being concentrated. The precipitate was collected and dried under vacuum at 40 °C for 24 h to get a red powder. Yield: 0.25 g, 42%. <sup>1</sup>H NMR (CDCl<sub>3</sub>, δ, ppm): 6.83–8.33 (m overlapped, 22H, H of benzene rings and triazole rings), 5.29 (s, 4H, triazole-CH<sub>2</sub>OCO), 4.21–4.75 (m overlapped, 12H, triazole-CH<sub>2</sub>CH<sub>2</sub>OCO and OCOCH<sub>2</sub>CH<sub>2</sub>OCOCH<sub>2</sub>), 3.62 (m overlapped, CH<sub>2</sub>N and CH<sub>2</sub> of PEG), 2.60 (m, 8H, OCOCH<sub>2</sub>CH<sub>2</sub>OCO), 1.32 (q, 24H, CH<sub>3</sub>) (see Figure S2 of Supporting Information).

## Results and Discussion

According to the molecule-design depicted in Figure 1, we presented the detailed synthetic route of fluorescent PRs, as



■ Scheme 1. Synthetic protocol of RhB-capped PRs via click chemistry.

shown in Scheme 1. The two terminal azido groups of  $N_3$ -PEG- $N_3$ , which are introduced into the ends of PEG chain by esterification of HO-PEG-OH with carboxylic azide, can react with RhB-alk in the end-capping reaction to give rise to the fluorescent PRs. As far as we know, RhB was used for the first time as the stopper of PRs. The fluorescence properties of the RhB stopper were quite different from that of the free molecule, especially the significant increase in the emission intensity. Thus, the fluorescent PR could work as a fluorescence-labeled giant carrier for drugs and biomolecules.<sup>[43,47]</sup> The threaded  $\alpha$ -CDs could work as the carrier and the location of the PR could be traced by fluorescence spectrometer. In this work, we only focus on the synthesis and characterization of the fluorescent PRs. The further modification and application will be reported later.

## Facile and Scalable Synthesis of Building Blocks for Click Coupling

One building block of the PRs was RhB-alk. RhB was extensively used as a fluorescent labeling reagent<sup>[48]</sup> and a source of laser dyes<sup>[49]</sup> because of its excellent properties, such as visible light excitation/emission, high fluorescence quantum yield. RhB was firstly treated with excess of propargyl alcohol to form RhB-alk, which could react efficiently with the azido groups of the axis to form the PRs. Azido-terminated polymers were very useful in the synthesis of polymer brushes,<sup>[36]</sup> star polymers,<sup>[34]</sup> and some other well-defined polymers by click reaction. Gao and Matyjaszewski have reported one novel synthetic routine for azido-terminated PEG by the nucleophilic substitution reaction between sodium azide and methanesulfonyl-terminated PEG.<sup>[36]</sup> The reaction process was versatile and the targeted product could be prepared in large scale as well. Herein, we developed an alternative route to readily synthesize  $N_3$ -PEG- $N_3$ , another building block of the PRs, via the facile DCC/DMAP condensation reaction between HO-PEG-OH and carboxylic azide. Notably, carboxylic azide could also be easily synthesized in large scale via the reaction between 2-azidoethanol and succinic anhydride. Carboxylic azide was once synthesized directly by nucleophilic substitution of carboxylic halides and sodium azide.<sup>[50]</sup> However, the yield was low, and more seriously, the releasing  $HN_3$  gas was extremely toxic and

dangerous during the collection of the product. Even though carboxylic azide was prepared via two-steps from 2-chloroethanol, sodium azide, and succinic anhydride, the total yield was quite high and it was easy to obtain large-scale pure product (up to sub-kilogram).

## Characterization of Building Blocks and Polyrotaxanes

The whole synthetic process of the PRs could be tracked by the NMR spectra (Figure 2). After ring-opening esterification of 2-azidoethanol, the proton peaks at 3.79 ( $CH_2OH$ ) and 3.44 ppm ( $N_3CH_2$ ) shift to 4.27 and 3.48 ppm respectively and the active proton peak of hydroxyl at 2.21 ppm vanishes while a new peak appears at 2.68 ppm for



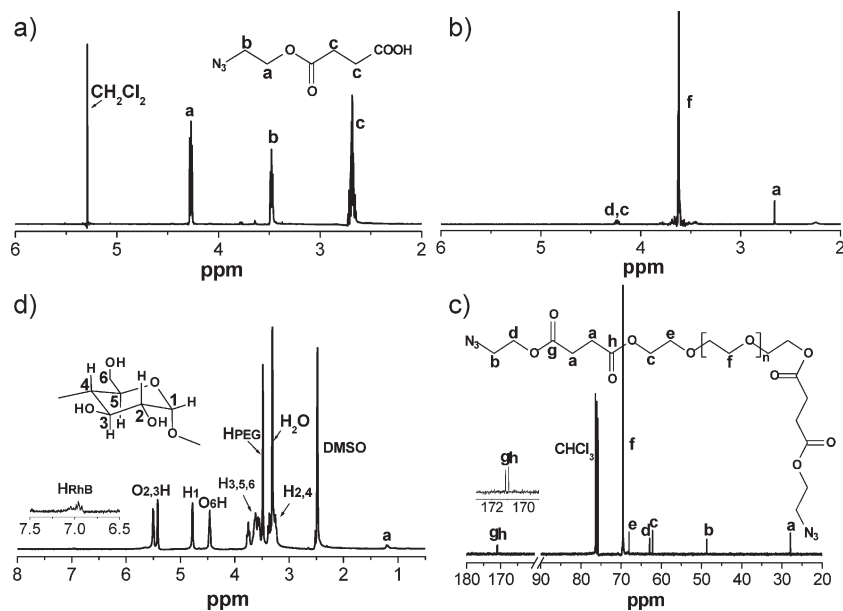


Figure 2. a)  $^1\text{H}$  NMR spectrum of carboxylic azide in  $\text{CDCl}_3$ , b)  $^1\text{H}$  NMR spectrum of  $\text{N}_3$ -PEG- $\text{N}_3$  in  $\text{CDCl}_3$ , c)  $^{13}\text{C}$  NMR spectrum of  $\text{N}_3$ -PEG- $\text{N}_3$  in  $\text{CDCl}_3$ , and d)  $^1\text{H}$  NMR spectrum of the PRs in  $\text{DMSO}-d_6$ . (b) and (c) shared the same chemical structure.

observed at  $1738\text{ cm}^{-1}$ . These variations of absorption peaks further confirmed the structures of building blocks and the PRs.

WAXD is one of the most powerful instruments to elucidate the structure of the inclusion complexes in the solid state and demonstrate the existence of pseudo-PRs and PRs.<sup>[51]</sup> The characteristic diffraction peak at  $2\theta = 20^\circ$  means the formation of columnar structure in the pseudo-PRs and the PRs. As shown in Figure 4, the diffraction peaks of the pseudo-PRs and the PRs at  $2\theta = 20^\circ$  are very strong and sharp (the little error was caused by the residue water), demonstrating the successful synthesis of the two compounds.

### Atomic Force Microscopy Observations

To observe the morphology of organic nanostructures such as brush-like nanocylinders and then ascertain their conformations on substrates are of particular importance to understand, manipulate, and apply them.<sup>[52]</sup> Previously, the scanning tunneling microscopy (STM) was utilized to observe the  $\alpha$ -CD beads of PRs.<sup>[53]</sup> Herein, we shifted our attention to AFM. AFM is easily available and compatible to any flat substrate and can work well in air and solvent.<sup>[54]</sup> To our delight, the fluorescent PRs can be observed as nanowire-like structures, as shown in Figure 5 (the color AFM images are shown in Figure S3 of

carboxylic azide ( $\text{OCOCH}_2\text{CH}_2\text{COOH}$ ) [Figure 2(a)], demonstrating the successful preparation of carboxylic azide. After esterification of HO-PEG-OH with carboxylic azide, two new peaks, peak a ( $\text{OCOCH}_2\text{CH}_2\text{COO}$ ) at 2.68 ppm and peak d ( $\text{N}_3\text{CH}_2\text{CH}_2\text{O}$ ) at 4.22 ppm, appear in the  $^1\text{H}$  NMR spectrum of  $\text{N}_3$ -PEG- $\text{N}_3$ , as shown in Figure 2(b). In the  $^{13}\text{C}$  NMR spectrum of  $\text{N}_3$ -PEG- $\text{N}_3$  [Figure 2(c)], there are two different carbonyl peaks around 171 ppm, signals g and h, which are in good accordance with two different carbonyl groups at the ends of  $\text{N}_3$ -PEG- $\text{N}_3$  chain. As to the other six peaks in Figure 2(c), peak f at 69.56 ppm is assigned to the carbon atoms of the PEG main chain and the other five peaks belong to the carbon atoms originally coming from carboxylic azide. Figure 2(d) shows the  $^1\text{H}$  NMR spectrum of the PRs. The group of peaks around 7.0 ppm is assigned to the hydrogen atoms of the benzene rings of RhB stopper and the peak at 1.20 ppm ( $\text{CH}_3$  of RhB, signal a) can also be utilized to calculate the number of the threaded  $\alpha$ -CDs per PR molecule in the following section of this article.

FT-IR spectra also gave clear evidence for the formation of targeted compounds, as shown in Figure 3. After esterification of HO-PEG-OH with carboxylic azide, the characteristic absorption peaks of azido and carbonyl groups of  $\text{N}_3$ -PEG- $\text{N}_3$  can be observed at  $2106$  and  $1738\text{ cm}^{-1}$ , respectively [Figure 3(b)]. In the FT-IR spectrum of the pseudo-PR [Figure 3(c)], the two peaks can still be found with a decreased intensity. In the FT-IR spectrum of the PRs [Figure 3(d)], the absorption peak at  $2106\text{ cm}^{-1}$  disappears due to the conversion of azido group in the end-capping reaction, while the peak of carbonyl group can still be

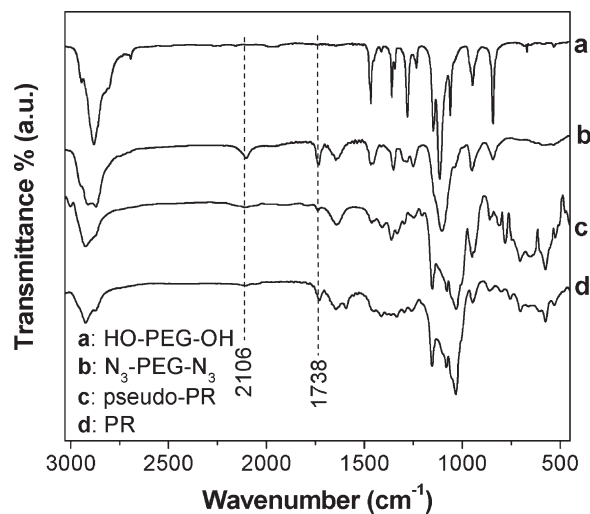


Figure 3. FT-IR spectra of a) HO-PEG-OH, b)  $\text{N}_3$ -PEG- $\text{N}_3$ , c) pseudo-PR, and d) PR.

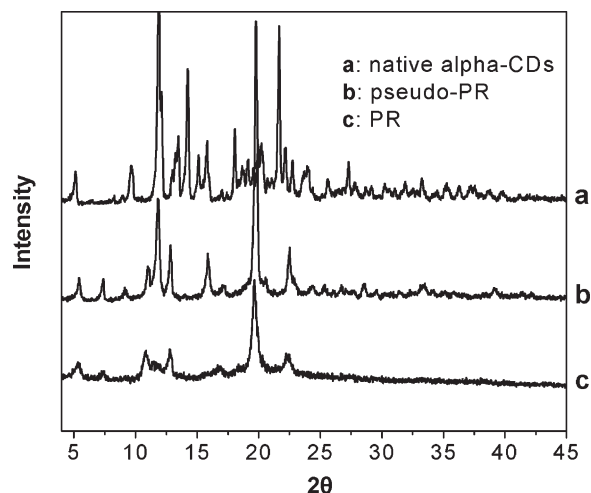


Figure 4. WAXD patterns of a) native  $\alpha$ -CD, b) pseudo-PR, and c) PR.

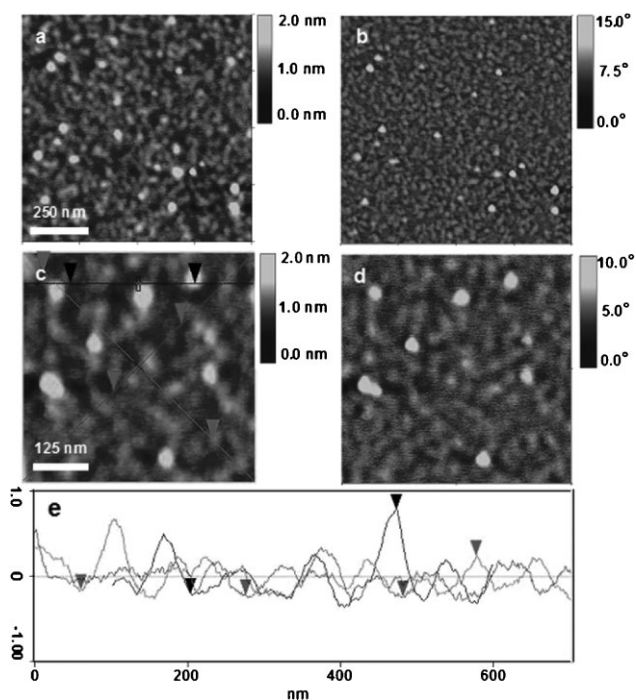


Figure 5. AFM images of the PRs on a mica wafer ( $4 \times 10^{-3} \text{ mg} \cdot \text{mL}^{-1}$ ): a) height image ( $1 \times 1 \mu\text{m}^2$ ), b) phase image of (a), c) amplified height image ( $500 \times 500 \text{ nm}^2$ ), d) phase image of (c), and e) section analysis of (c).

Supporting Information). According to the surface plot [Figure 5(e)], the average vertical distance between the peak and the bottom is  $0.41 \pm 0.10 \text{ nm}$ , which is smaller than the diameter of an ideal PR nanorod, ca.  $1.4 \text{ nm}$ . This phenomenon might be caused by the flattened conformation of  $\alpha$ -CD on a substrate and the exposure of the partially threaded PEG axis to the probe during AFM analysis.<sup>[55]</sup> The

Table 1. Four methods to calculate the value of  $N_{\text{CD}}$  and the corresponding results.

Method	NMR	GPC	UV-Vis	Fluorescence
$N_{\text{CD}}^{\text{a)}$	15.0	15.1	10.6	16.9

<sup>a)</sup>The number of  $\alpha$ -CDs of each PR molecule.

obtained average vertical distance is the numerical average of  $\alpha$ -CD and PEG diameters. Though the concentration of the PR solution is very low, ca.  $4 \times 10^{-3} \text{ mg} \cdot \text{mL}^{-1}$ , the strong aggregation inclination of the PR molecules via the hydrogen bonds can hardly be avoided. The lengths of most observed features are around  $100 \text{ nm}$  and larger aggregations exist as well, in wide-field image of the PR [Figure 5(a)]. If the concentration of the AFM sample was higher (ca.  $0.2 \text{ mg} \cdot \text{mL}^{-1}$ ), we could only see some huge aggregated structures of the PRs (see Figure S4 of Supporting Information).

#### Cyclodextrin-Number Detection of Polyrotaxane

The number of  $\alpha$ -CDs of each PR supermolecule ( $N_{\text{CD}}$ ) is also a very important parameter for the characterization of PRs. Herein, we developed four different methods to obtain the value of  $N_{\text{CD}}$ . The results are shown in Table 1 and the calculation formulas are listed in the appendix of the Supporting Information.

First,  $N_{\text{CD}}$  was calculated from the integral area of the peak assigned to the H1 of  $\alpha$ -CD and that of signal a (proton peak assigned to the methyl groups of RhB stopper) in  $^1\text{H}$  NMR spectrum [Figure 2(d)]. The calculated result was 15.0.

DMSO is known as the only good organic solvent for most of the unmodified PRs. In order to determine the molecular weight of the fluorescent PR by GPC with DMF, the PR was treated with valeryl chloride to improve its solubility. In the  $^1\text{H}$  NMR spectrum of PR-vc (see Figure S1 of Supporting Information), almost all hydroxyl groups of the PRs are capped by the chloride.  $\overline{M}_n$  of PR-vc was 43 600 and the polydispersity index (PDI) was 1.13. As a result, the value of  $N_{\text{CD}}$  was 15.1, which was quite close to the result gotten via NMR method (15.0 therein).

Harada et al.<sup>[56]</sup> first used UV-Vis data to calculate the value of  $N_{\text{CD}}$  and the result was quite consistent with that gotten via GPC. Extinction coefficient of the stopper of the PRs was the key parameter to calculate the value of  $N_{\text{CD}}$  via UV-Vis method. We compared the extinction coefficients of the three related RhB derivatives, neat RhB, RhB-alk, and RhB-PEG-RhB, in DMSO and alkaline aqueous solution, in order to decide which one was the best substitute of the stopper. To get the extinction coefficients in alkaline aqueous solution, all compounds were dissolved in  $1 \text{ M}$

**Table 2.** The values of  $N_{CD}$  resulting from the UV–Vis extinction coefficients of neat RhB, RhB-alk, RhB-PEG-RhB, and PR in DMSO and alkaline aqueous solution.<sup>a)</sup>

Compound	DMSO		Water	
	$\epsilon^{b)}$	$N_{CD}^{c)}$	$\epsilon$	$N_{CD}$
	$10^4 \text{ L} \cdot \text{mol}^{-1} \cdot \text{cm}^{-1}$		$10^4 \text{ L} \cdot \text{mol}^{-1} \cdot \text{cm}^{-1}$	
RhB	2.07	3.5	4.98	6.9
RhB-alk	3.55	10.6	4.91	6.7
RhB-PEG-RhB	15.5	66.3	18.1	41.3
PR	3.35 <sup>d)</sup>	–	8.26 <sup>d)</sup>	–

<sup>a)</sup>As to the UV–Vis standard lines, see Figure S5 and S6 of Supporting Information; <sup>b)</sup>UV–Vis extinction coefficient; <sup>c)</sup>The number of  $\alpha$ -CDs of each PR molecule; <sup>d)</sup>The number of  $\alpha$ -CDs of each PR molecule was assumed to be 15.0.

NaOH aqueous solution and diluted by buffer solution (pH = 10.5) to avoid the precipitation of the PRs and the influence of pH on absorption intensity during the whole measurement. The value of  $N_{CD}$  was assumed as 15.0 (considering the results gotten by NMR and GPC methods) in order to calculate the extinction coefficients of the PR inversely. The corresponding results are listed in Table 2.

According to Table 2, the extinction coefficient of RhB-alk in DMSO solution,  $3.55 \times 10^4 \text{ L} \cdot \text{mol}^{-1} \cdot \text{cm}^{-1}$ , was quite close to the assumed one of the PRs ( $3.35 \times 10^4 \text{ L} \cdot \text{mol}^{-1} \cdot \text{cm}^{-1}$ ); so it could be utilized to calculate the value of  $N_{CD}$  and the corresponding result was 10.6. The result was distinctly smaller than those gotten via NMR and GPC method. The reason might be the different structures and chemical environments of the two kinds of chromophores. The difference of the wavelengths of the absorption peaks in the UV–Vis spectra was a good evidence for the discrepancy of the RhB derivatives. As shown in Figure 6, we compared the wavelengths of the absorption peaks of neat RhB, the mixture with the same composition of the PR (the mole ratio of  $N_3$ -PEG- $N_3$ , RhB-alk, and  $\alpha$ -CDs was 1:2:15), the mixture of  $\alpha$ -CDs and RhB-PEG-RhB (the mole ratio of RhB-PEG-RhB and  $\alpha$ -CDs was 1:15), and the PRs in DMSO solution. The absorption peaks of the former three were all at 564 nm, while that of the PR slightly moved to 567 nm. The result also demonstrated the successful synthesis of the PRs (not the mixture of  $N_3$ -PEG- $N_3$ , RhB-alk, and  $\alpha$ -CDs).

$N_{CD}$  could also be calculated through the fluorescence emission coefficient gotten from fluorescence spectra. Herein, fluorescence spectrum was utilized for the first time as a novel method to calculate the value of  $N_{CD}$ . Similar with UV–Vis method, the emission coefficients of the three related RhB derivatives are all listed in Table 3. The fluorescence emission coefficient of RhB-PEG-RhB in DMSO solution,  $1.46 \times 10^9 \text{ L} \cdot \text{mol}^{-1} \cdot \text{cm}^{-1}$ , was the closest one to that of the PRs ( $1.29 \times 10^9 \text{ L} \cdot \text{mol}^{-1} \cdot \text{cm}^{-1}$ ), so it could be used to calculate the value of  $N_{CD}$  and the corresponding result was 16.9. This value is also very close to that obtained

from GPC or NMR method, indicating that fluorescence method would be an alternative technique to determine  $N_{CD}$ .

### Unique Fluorescence Properties of the Polyrotaxanes

The fluorescence emission intensities at 590 nm were utilized to draw the plots of emission intensity as a function of fluorophores concentration (see Figure 7, the color photographs of the excited PRs are shown in Figure S7 of Supporting Information). Interestingly, dramatically different plots were found. As shown in Figure 8(a), the emission intensity of neat RhB in DMSO solution is around zero until the concentration of RhB rises to a certain point (the threshold concentration is ca.  $1.6 \times 10^{-5} \text{ mol} \cdot \text{L}^{-1}$ ); while above the threshold concentration, the emission

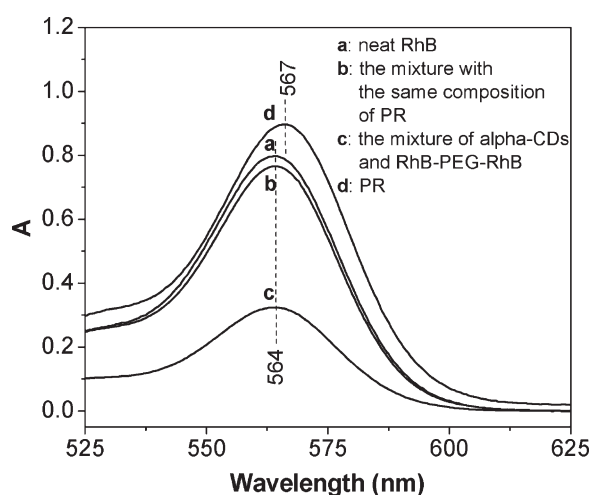


**Figure 6.** UV–Vis spectra of a) neat RhB, b) the mixture with the same composition of PR (the molar ratio of  $N_3$ -PEG- $N_3$ , RhB-alk, and  $\alpha$ -CDs was 1:2:15), c) the mixture of  $\alpha$ -CDs and RhB-PEG-RhB (the molar ratio of RhB-PEG-RhB and  $\alpha$ -CDs was 1:15), and d) PR in DMSO solution.

**Table 3.** The values of  $N_{CD}$  resulting from the fluorescence emission coefficients of neat RhB, RhB-alk, RhB-PEG-RhB, and PR in DMSO and alkaline aqueous solution.

Compound	DMSO		Water	
	$\epsilon'$ <sup>a)</sup>	$N_{CD}$ <sup>b)</sup>	$\epsilon'$	$N_{CD}$
	$10^8 \text{ L} \cdot \text{mol}^{-1} \cdot \text{cm}^{-1}$		$10^8 \text{ L} \cdot \text{mol}^{-1} \cdot \text{cm}^{-1}$	
RhB	— <sup>c)</sup>	— <sup>c)</sup>	7.91	8.0
RhB-alk	3.38	— <sup>d)</sup>	5.49	3.7
RhB-PEG-RhB	14.6	16.9	20.6	30.7
PR	12.9 <sup>e)</sup>	—	13.9 <sup>e)</sup>	—

<sup>a)</sup>Fluorescence emission coefficient; <sup>b)</sup>The number of  $\alpha$ -CDs of each PR molecule; <sup>c)</sup>The fluorescence emission coefficient of RhB in DMSO solution was not available and the resulting  $N_{CD}$  was not available either because the plot of concentration versus emission intensity is not linear as shown in Figure 8(a); <sup>d)</sup>The value of the resulting  $N_{CD}$  was negative, indicating that RhB-alk is not suitable for the calculation of  $N_{CD}$ ; <sup>e)</sup>The number of  $\alpha$ -CDs of each PR molecule was assumed to be 15.0.

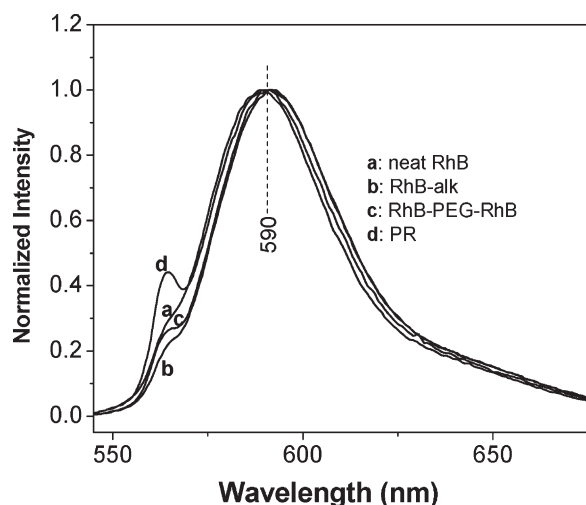


**Figure 7.** Fluorescence emission spectra of a) neat RhB, b) RhB-alk, c) RhB-PEG-RhB, and d) PR in DMSO solution. All the fluorescence emission spectra were excited at 564 nm and normalized.

intensity increases fast and almost linearly with the increase of fluorophores concentration. In contrast, linear plots were found for RhB-alk, RhB-PEG-RhB, and the PRs (the value of  $N_{CD}$  was assumed as 15.0) in the whole tested range of concentration. The slope of the fit line of RhB-alk was smaller than that of the fit line of RhB-PEG-RhB, whereas the plot of the PRs was almost overlapped with that of RhB-PEG-RhB. The corresponding emission coefficients of RhB-alk, RhB-PEG-RhB, and the PRs are calculated as  $3.38 \times 10^8$ ,  $1.46 \times 10^9$ , and  $1.29 \times 10^9 \text{ L} \cdot \text{mol}^{-1} \cdot \text{cm}^{-1}$  respectively (Table 3).

Similar result was achieved in alkaline aqueous solution, as shown in Figure 9 (all the samples were excited at 553 nm

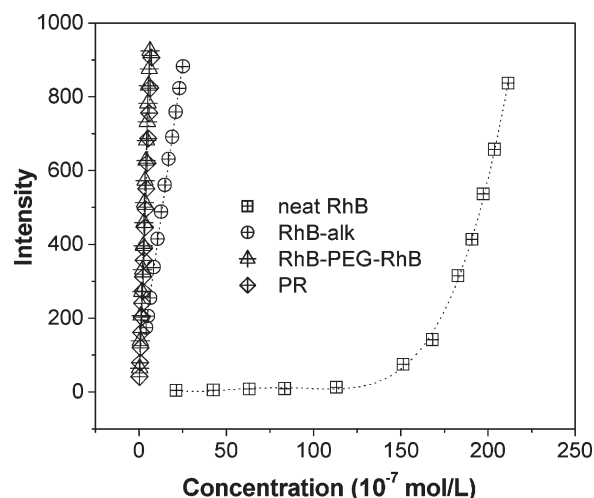


**Figure 8.** Fluorophores concentration versus fluorescence emission intensity plots of neat RhB, RhB-alk, RhB-PEG-RhB, and PR ( $N_{CD}$  was assumed as 15.0) in DMSO solution. All the fluorescence emission spectra were excited at 564 nm and the emission peak points were at 590 nm.

and the emission peak points were at 577 nm; see Figure S8 of Supporting Information). The fluorophores concentration versus fluorescence emission intensity plots of the four kinds of compounds were all linear and the calculated emission coefficients were  $7.91 \times 10^8$  for neat RhB,  $5.49 \times 10^8$  for RhB-alk,  $2.06 \times 10^9$  for RhB-PEG-RhB, and  $1.39 \times 10^9 \text{ L} \cdot \text{mol}^{-1} \cdot \text{cm}^{-1}$  for the PR, respectively, as listed in Table 3.

In short, the order of the fluorescence emission coefficients of the four kinds of molecules in the same solvent was RhB, RhB-alk < PR < RhB-PEG-RhB.

Such a fluorescence enhancement phenomenon could be explained by the different local environments of RhB



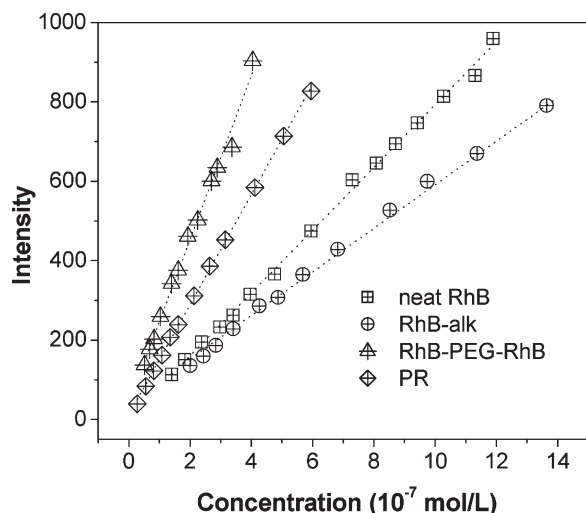


**Figure 9.** Fluorophores concentration versus fluorescence emission intensity plots of neat RhB, RhB-alk, RhB-PEG-RhB, and PR ( $N_{CD}$  was assumed to be 15.0) in alkaline aqueous solution. All the fluorescence emission spectra were excited at 553 nm and the emission peak points were at 577 nm.

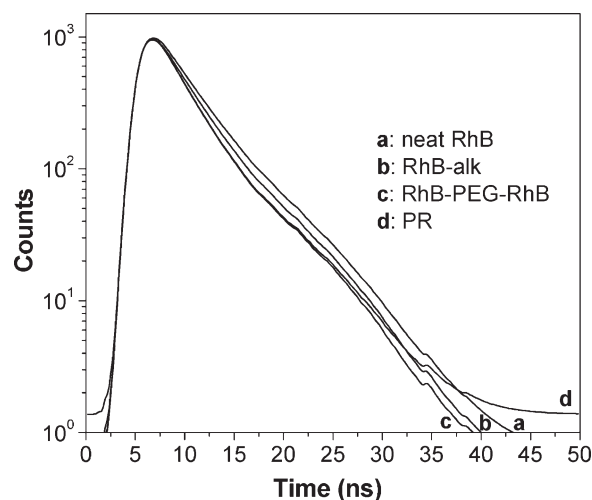


**Figure 10.** Fluorescence lifetime fit curves of a) neat RhB, b) RhB-alk, c) RhB-PEG-RhB, and d) PR in DMSO. All samples were excited at 564 nm and the emission peak points were at 590 nm. The excitation and emission slit widths were both 15 nm.

fluorophores. It is known that the fluorescence quantum yield of RhB increases with decreasing polarity of the medium.<sup>[57]</sup> The rotaxane parts of the PRs hindered the interaction between RhB fluorophores and the solvent molecules, and hence, the RhB fluorophores were embedded in a rather lower polar environment, resulting in the increase of fluorescence emission intensity.<sup>[58]</sup> As to the more flexible PEG parts of RhB-PEG-RhB, the RhB fluorophores were embedded more tightly, so the fluorescence intensity of RhB-PEG-RhB was even higher than that of the PRs under the same condition. Nevertheless, more studies in both experiments and theoretical simulation were required to totally uncover the reason of this phenomenon in the future.

Fluorescence lifetime ( $\tau_0$ ) is a very useful parameter to measure the different molecular structures, chemical reactions, and local environments of different kinds of molecules.<sup>[59]</sup> As shown in Figure 10, the fluorescence lifetime fit curves of RhB-PEG-RhB and the PR in DMSO are almost overlapped and this phenomenon furnishes an extra evidence for the similar chemical structure and local environment of the two kinds of RhB fluorophores (as to fluorescence decay curves, see Figure S9 of Supporting Information). The Strickler–Berg equation in ref. [60] showed the relationship between absorption intensity and fluorescence lifetime:

$$1/\tau_0 = 2.880 \times 10^{-9} n^2 \langle \tilde{\nu}_f^{-3} \rangle_{Av}^{-1} \frac{g_l}{g_u} \int \epsilon d \ln \tilde{\nu} \quad (1)$$

$$\langle \tilde{\nu}_f^{-3} \rangle_{Av}^{-1} = \frac{\int I(\tilde{\nu}) d\tilde{\nu}}{\int \tilde{\nu}^{-3} I(\tilde{\nu}) d\tilde{\nu}} \quad (2)$$

In this equation,  $\tau_0$  is the fluorescence lifetime;  $n$  is the refractive index of the medium;  $\tilde{\nu}$  is the frequency of the transition in  $\text{cm}^{-1}$ ;  $I(\tilde{\nu})$  is the intensity at certain frequency;  $g_l$  and  $g_u$  are the degeneracies of the lower and upper energy states;  $\epsilon$  is the molar extinction coefficient.

According to this equation, the fluorescence lifetime would decrease with the increasing extinction coefficient of the fluorophores in the same solvent when all the other parameters remain unchanged. In DMSO solution, the fluorescence lifetime of neat RhB (3.59 ns) was longer than those of RhB-alk (3.31 ns) and RhB-PEG-RhB (2.99 ns), while the extinction coefficient of neat RhB ( $2.07 \times 10^4 \text{ L} \cdot \text{mol}^{-1} \cdot \text{cm}^{-1}$ ) was lower than those of RhB-alk ( $3.55 \times 10^4 \text{ L} \cdot \text{mol}^{-1} \cdot \text{cm}^{-1}$ ) and RhB-PEG-RhB ( $1.55 \times 10^5 \text{ L} \cdot \text{mol}^{-1} \cdot \text{cm}^{-1}$ ). Such a result was quite in accordance with the conclusion given by ref. [61]. The fluorescence lifetime of the PRs was the same as that of RhB-PEG-RhB, 2.99 ns as well, which might be mainly affected by other structure related parameters, for instance, the frequency of the transition or the degeneracies of the lower and upper energy states of the fluorophores.

## Conclusion

In summary, we synthesized one kind of fluorescent PRs based on PEG,  $\alpha$ -CDs and RhB derivative stoppers via an

azide–alkyne click reaction. The click reaction was demonstrated to take place fast enough, to ensure the successful synthesis of the PRs. The building blocks with azido or alkyne groups can be widely applied to construct other versatile structures and nanomaterials. AFM was proven to be a powerful characterization tool to observe the PR nanostructures at a suitable concentration, and a nano-wire-like morphology with a resolution of less than 1 nm was viewed. We also found that the fluorescence emission intensities of RhB-PEG-RhB and the PRs were obviously higher than those of RhB-alk and neat RhB with the same RhB fluorophores concentrations in both DMSO and aqueous solution. The novel fluorescent enhancement property of the PR would be useful in application in biological fields, such as dye labeled drug carriers, because the existence of the fluorescent PRs could be detected by the fluorescence spectrometer with a rather low concentration. Also, the PR was one kind of biodegradable PRs, since the ester groups bonding to the PEG axis could be hydrolyzed to release the efficient drug carriers ( $\alpha$ -CDs), if required. The biological application of the fluorescent PRs is still under study and might be reported in the near future.

## Appendix

### The Calculation Formulas of Four methods to Calculate the Value of $N_{CD}$

$$N_{CD} = \frac{4I_1}{I_r} \quad (3)$$

Wherein  $I_1$  was the integral area of the peak of the H1 of  $\alpha$ -CD and  $I_r$  was that of signal a (proton peak assigned to the methyl groups of RhB stopper) in  $^1\text{H}$  NMR spectrum (Figure 2d).

$$N_{CD} = \frac{M_n - 2M_{RhB} - M_{N_3-PEG-N_3}}{M'_{\alpha-CD}} \quad (4)$$

Wherein  $M_{RhB}$  ( $517.07 \text{ g} \cdot \text{mol}^{-1}$ ),  $M_{N_3-PEG-N_3}$  ( $4938 \text{ g} \cdot \text{mol}^{-1}$ ) and  $M'_{\alpha-CD}$  ( $2486.10 \text{ g} \cdot \text{mol}^{-1}$ ) designated the molecular weights of RhB-alk,  $N_3$ -PEG- $N_3$ , and valeryl chloride modified  $\alpha$ -CD bead, respectively.

When 4.9 mg PRs was dissolved in 24.05 mL DMSO, the maximum absorption value of the PR ( $A_p$ ) was 0.8964 at 567 nm (Figure 6d). The calculation formula was shown as follow:

$$n_{RhB} = \frac{A_p \times V_p}{\epsilon} \quad (5)$$

$$N_{CD} = \frac{2m_p - n_{RhB} \cdot (2M_{RhB} + M_{N_3-PEG-N_3})}{M_{\alpha-CD} \cdot n_{RhB}} \quad (6)$$

Wherein  $V_p$  was the volume of the solution of the PR (24.05 mL) and  $m_p$  was the weight of the PR in the solution (4.9 mg).  $M_{RhB}$  ( $517.07 \text{ g} \cdot \text{mol}^{-1}$ ),  $M_{N_3-PEG-N_3}$  ( $4938 \text{ g} \cdot \text{mol}^{-1}$ ), and  $M_{\alpha-CD}$  ( $972.84 \text{ g} \cdot \text{mol}^{-1}$ ) were the molecular weights of RhB-alk,  $N_3$ -PEG- $N_3$ , and  $\alpha$ -CD, respectively.

$$n'_{RhB} = \frac{I_p \times V_0 \times (V_1 + V_2)}{\epsilon' V_1} \quad (7)$$

$$N_{CD} = \frac{2m'_p - n'_{RhB} \cdot (2M_{RhB} + M_{N_3-PEG-N_3})}{M_{\alpha-CD} \cdot n'_{RhB}} \quad (8)$$

When 1.6 mg ( $m'_p$ ) PRs was dissolved in 25.00 mL ( $V_0$ ) DMSO to form a concentrated solution of the PRs and then 0.10 mL ( $V_1$ ) concentrated PRs solution was diluted with 20.00 mL ( $V_2$ ) DMSO, the fluorescence emission intensity of the diluted solution was 41.45 ( $I_p$ ). The values of  $M_{N_3-PEG-N_3}$ ,  $M_{\alpha-CD}$ , and  $M_{RhB}$  were the same as those for UV/Vis method.

**Acknowledgements:** This work was supported by the *National Natural Science Foundation of China* (no. 50773038), *National Basic Research Program of China* (973 Program) (no. 2007CB936000), *Science and Technology Commission of Shanghai Municipality* (07pj14048), the *Foundation for the Author of National Excellent Doctoral Dissertation of China* (no. 200527), and the *Program for New Century Excellent Talents in University of China*.

Received: June 11, 2009; Accepted: July 28, 2009; Published online: September 8, 2009; DOI: 10.1002/macp.200900281

**Keywords:** atomic force microscopy; click chemistry; cyclodextrin; fluorescence; polyrotaxane

- [1] [1a] A. Harada, M. Kamachi, *Macromolecules* **1990**, *23*, 2821; [1b] A. Harada, J. Li, M. Kamachi, *Macromolecules* **1993**, *26*, 5698; [1c] A. Harada, J. Li, M. Kamachi, *Nature* **1992**, *356*, 325; [1d] A. Harada, Y. Takashima, H. Yamaguchi, *Chem. Soc. Rev.* **2009**, *38*, 875.
- [2] [2a] J. Araki, K. Ito, *Soft Matter* **2007**, *3*, 1456; [2b] F. Huang, H. W. Gibson, *Prog. Polym. Sci.* **2005**, *30*, 982; [2c] S. Loethen, J.-M. Kim, D. H. Thompson, *Polym. Rev.* **2007**, *47*, 383; [2d] A. Harada, *J. Polym. Sci., Part A: Polym. Chem.* **2006**, *44*, 5113; [2e] G. Wenz, B.-H. Han, A. Müller, *Chem. Rev.* **2006**, *106*, 782.

- [3] [3a] Y. Okumura, K. Ito, *Adv. Mater.* **2001**, *13*, 485; [3b] T. Karino, Y. Okumura, K. Ito, M. Shibayama, *Macromolecules* **2004**, *37*, 6177.
- [4] T. Ooya, H. Mori, M. Terano, N. Yui, *Macromol. Rapid Commun.* **1995**, *16*, 259.
- [5] [5a] A. Harada, J. Li, M. Kamachi, *Nature* **1993**, *364*, 516; [5b] M. Ceccato, P. J. Nostro, C. Rossi, C. Bonechi, A. Donati, P. Baglioni, *J. Phys. Chem. B* **1997**, *101*, 5094.
- [6] [6a] M. J. Frampton, H. L. Anderson, *Angew. Chem., Int. Ed.* **2007**, *46*, 1028; [6b] N. Yui, T. Ooya, *Chem. Eur. J.* **2006**, *12*, 6730.
- [7] A. Harada, J. Li, M. Kamachi, *J. Am. Chem. Soc.* **1994**, *116*, 3192.
- [8] N. Yui, T. Ooya, T. Kumeno, *Bioconjugate Chem.* **1998**, *9*, 118.
- [9] H. Fujita, T. Ooya, N. Yui, *Polym. J.* **1999**, *31*, 1099.
- [10] M. Tamura, A. Ueno, *Chem. Lett.* **1998**, *27*, 369.
- [11] J. Araki, C. M. Zhao, K. Ito, *Macromolecules* **2005**, *38*, 7524.
- [12] T. Ooya, H. S. Choi, A. Yamashita, N. Yui, Y. Sugaya, A. Kano, A. Maruyama, H. Akita, R. Ito, K. Kogure, H. Harashima, *J. Am. Chem. Soc.* **2006**, *128*, 3852.
- [13] M. Okada, A. Harada, *Macromolecules* **2003**, *36*, 9701.
- [14] [14a] T. Ooya, N. Yui, *J. Controlled Release* **1999**, *58*, 251; [14b] T. Ichi, J. Watanabe, T. Ooya, N. Yui, *Biomacromolecules* **2001**, *2*, 204; [14c] M. Eguchi, T. Ooya, N. Yui, *J. Controlled Release* **2004**, *96*, 301; [14d] M. Kidowaki, T. Nakajima, J. Araki, A. Inomata, H. Ishibashi, K. Ito, *Macromolecules* **2007**, *40*, 6859; [14e] T. Arai, M. Hayashi, N. Takagi, T. Takata, *Macromolecules* **2009**, *42*, 1881.
- [15] [15a] M. Kidowaki, C. Zhao, T. Kataoka, K. Ito, *Chem. Commun.* **2006**, 4102; [15b] T. Kataoka, M. Kidowaki, C. Zhao, H. Minamikawa, T. Shimizu, K. Ito, *J. Phys. Chem. B* **2006**, *110*, 24377.
- [16] [16a] S. Samitsu, J. Araki, T. Kataoka, K. Ito, *J. Polym. Sci., Part B: Polym. Phys.* **2006**, *44*, 1985; [16b] J. Araki, K. Ito, *J. Polym. Sci., Part A: Polym. Chem.* **2006**, *44*, 6312; [16c] J. Araki, T. Kataoka, K. Ito, *J. Appl. Polym. Sci.* **2007**, *105*, 2265.
- [17] [17a] T. Sakai, H. Murayama, S. Nagano, Y. Takeoka, M. Kidowaki, K. Ito, T. Seki, *Adv. Mater.* **2007**, *19*, 2023; [17b] T. Karino, Y. Okumura, C. Zhao, M. Kidowaki, T. Kataoka, K. Ito, M. Shibayama, *Macromolecules* **2006**, *39*, 9435.
- [18] T. Zhao, H. W. Beckham, *Macromolecules* **2003**, *36*, 9859.
- [19] L. Ren, F. Ke, Y. Chen, D. Liang, J. Huang, *Macromolecules* **2008**, *41*, 5295.
- [20] F. Cacialli, J. S. Wilson, J. J. Michels, C. Daniel, C. Silva, R. H. Friend, N. Severin, P. Samori, J. P. Rabe, M. J. O'Connell, P. N. Taylor, H. L. Anderson, *Nat. Mater.* **2002**, *1*, 160.
- [21] M. Tamura, A. Ueno, *Bull. Chem. Soc. Jpn.* **2000**, *73*, 147.
- [22] N. Jarroux, P. Guban, H. Cheradame, L. Auvray, *J. Phys. Chem. B* **2005**, *109*, 23816.
- [23] H. Yu, Z. Feng, A. Zhang, D. Hou, L. Sun, *Polymer* **2006**, *47*, 6066.
- [24] [24a] G. Wenz, B. Keller, *Angew. Chem., Int. Ed.* **1992**, *31*, 197; [24b] G. Wenz, *Angew. Chem., Int. Ed.* **1994**, *33*, 803.
- [25] H. Murayama, A. B. Imran, S. Nagano, T. Seki, M. Kidowaki, K. Ito, Y. Takeoka, *Macromolecules* **2008**, *41*, 1808.
- [26] M. Tamura, D. Gao, A. Ueno, *Chem. Eur. J.* **2001**, *7*, 1390.
- [27] H. C. Kolb, M. G. Finn, K. B. Sharpless, *Angew. Chem., Int. Ed.* **2001**, *40*, 2004.
- [28] O. Altintas, G. Hizal, U. Tunca, *J. Polym. Sci., Part A: Polym. Chem.* **2006**, *44*, 5699.
- [29] D. E. Bergbreiter, B. S. Chance, *Macromolecules* **2007**, *40*, 5337.
- [30] J. A. Opsteen, R. P. Brinkhuis, R. L. M. Teeuwen, D. W. P. M. Löwik, J. C. M. van Hest, *Chem. Commun.* **2007**, 3136.
- [31] P. Wu, A. K. Feldman, A. K. Nugent, C. J. Hawker, A. Scheel, B. Voit, J. Pyun, J. M. J. Fréchet, K. B. Sharpless, V. V. Fokin, *Angew. Chem., Int. Ed.* **2004**, *43*, 3928.
- [32] A. J. Scheel, H. Komber, B. Voit, *Macromol. Rapid Commun.* **2004**, *25*, 1175.
- [33] N. V. Tsarevsky, B. S. Sumerlin, K. Matyjaszewski, *Macromolecules* **2005**, *38*, 3558.
- [34] H. Gao, K. Matyjaszewski, *Macromolecules* **2006**, *39*, 4960.
- [35] B. S. Sumerlin, N. V. Tsarevsky, G. Louche, R. Y. Lee, K. Matyjaszewski, *Macromolecules* **2005**, *38*, 7540.
- [36] H. Gao, K. Matyjaszewski, *J. Am. Chem. Soc.* **2007**, *129*, 6633.
- [37] J. Xu, J. Ye, S. Liu, *Macromolecules* **2007**, *40*, 9103.
- [38] J. Zhang, Y. Zhou, Z. Zhu, Z. Ge, S. Liu, *Macromolecules* **2008**, *41*, 1444.
- [39] H. He, Y. Zhang, C. Gao, J. Wu, *Chem. Commun.* **2009**, 1655.
- [40] Y. Zhang, H. He, C. Gao, *Macromolecules* **2008**, *41*, 9581.
- [41] [41a] W. R. Dichtel, O. S. Miljanić, J. M. Spruell, J. R. Heath, J. F. Stoddart, *J. Am. Chem. Soc.* **2006**, *128*, 10388; [41b] V. Aucagne, K. D. Hänni, D. A. Leigh, P. J. Lusby, D. B. Walker, *J. Am. Chem. Soc.* **2006**, *128*, 2186.
- [42] S. Loethen, T. Ooya, H. S. Choi, N. Yui, D. H. Thompson, *Biomacromolecules* **2006**, *7*, 2501.
- [43] [43a] B. N. G. Giepmans, S. R. Adams, M. H. Ellisman, R. Y. Tsien, *Science* **2006**, *312*, 217; [43b] S. Weiss, *Science* **1999**, *283*, 1676.
- [44] C. Gao, H. He, L. Zhou, X. Zheng, Y. Zhang, *Chem. Mater.* **2009**, *21*, 360.
- [45] X.-M. Liu, A. Thakur, D. Wang, *Biomacromolecules* **2007**, *8*, 2653.
- [46] J. Araki, K. Ito, *J. Polym. Sci., Part A: Polym. Chem.* **2006**, *44*, 532.
- [47] B. Schuler, E. A. Lipman, W. A. Eaton, *Nature* **2002**, *419*, 743.
- [48] [48a] K. Glunde, C. A. Foss, T. Takagi, F. Wildes, Z. M. Bhujwalla, *Bioconjugate Chem.* **2005**, *16*, 843; [48b] L. B. Poole, C. Klomsiri, S. A. Knaggs, C. M. Furdui, K. J. Nelson, M. J. Thomas, J. S. Fetrow, L. W. Daniel, S. B. King, *Bioconjugate Chem.* **2007**, *18*, 2004; [48c] T. W. Loo, D. M. Clarke, *J. Biol. Chem.* **2002**, *277*, 44332.
- [49] O. G. Peterson, J. P. Webb, W. C. Mccolgin, J. H. Eberly, *J. Appl. Phys.* **1971**, *42*, 1917.
- [50] C. Grandjean, A. Boutonnier, C. Guerreiro, J.-M. Fournier, L. A. Mulard, *J. Org. Chem.* **2005**, *70*, 7123.
- [51] [51a] I. N. Topchieva, A. E. Tonelli, I. G. Panova, E. V. Matuchina, F. A. Kalashnikov, V. Gerasimov, C. C. Rusa, M. Rusa, M. A. Hunt, *Langmuir* **2004**, *20*, 9036; [51b] J. Li, D. Yan, *Macromolecules* **2001**, *34*, 1542; [51c] X. Zhu, L. Chen, D. Yan, Q. Chen, Y. Yao, Y. Xiao, J. Hou, J. Li, *Langmuir* **2004**, *20*, 484.
- [52] [52a] C. K. Ober, S. Z. D. Cheng, P. T. Hammond, M. Muthukumar, E. Reichmanis, K. L. Wooley, T. P. Lodge, *Macromolecules* **2009**, *42*, 465; [52b] S. S. Sheiko, B. S. Sumerlin, K. Matyjaszewski, *Prog. Polym. Sci.* **2008**, *33*, 759.
- [53] H. Shigekawa, K. Miyake, J. Sumaoka, A. Harada, M. Komiyama, *J. Am. Chem. Soc.* **2000**, *122*, 5411.
- [54] [54a] S. J. Lord, S. S. Sheiko, I. LaRue, H. Lee, K. Matyjaszewski, *Macromolecules* **2004**, *37*, 4235; [54b] J. Yuan, Y. Xu, A. Walther, S. Bolisetty, M. Schumacher, H. Schmalz, M. Ballauff, A. H. E. Müller, *Nat. Mater.* **2008**, *7*, 718.
- [55] M. van den Boogaard, G. Bonnet, P. van't Hof, Y. Wang, C. Brochon, P. van Hutten, A. Lapp, G. Hadziioannou, *Chem. Mater.* **2004**, *16*, 4383.
- [56] A. Harada, J. Li, T. Nakamitsu, M. Kamachi, *J. Org. Chem.* **1993**, *58*, 7524.
- [57] [57a] G. Jones II, W. R. Jackson, C. Y. Choi, W. R. Bergmark, *J. Phys. Chem.* **1985**, *89*, 294; [57b] T.-L. Chang, H. C. Cheung,

- J. Phys. Chem.* **1992**, *96*, 4874; [57c] R. S. Moog, M. D. Ediger, S. G. Boxer, M. D. Fayer, *J. Phys. Chem.* **1982**, *86*, 4694; [57d] K. G. Casey, E. L. Quitevis, *J. Phys. Chem.* **1988**, *92*, 6590.
- [58] Y. Shiraishi, R. Miyamoto, X. Zhang, T. Hirai, *Org. Lett.* **2007**, *9*, 3921.
- [59] [59a] M. Wilhelm, C. L. Zhao, Y. Wang, R. Xu, M. A. Winnik, J. L. Mura, G. Riess, M. D. Croucher, *Macromolecules* **1991**, *24*, 1033; [59b] A. G. Szabo, D. M. Rayner, *J. Am. Chem. Soc.* **1980**, *102*, 554; [59c] A. Szabo, *J. Chem. Phys.* **1984**, *81*, 150.
- [60] S. J. Strickler, R. A. Berg, *J. Chem. Phys.* **1962**, *37*, 814.
- [61] [61a] H. A. S. Al-Shamiri, M. T. H. Abou Kana, I. M. Azzouz, Y. A. Badr, *Opt. Laser Technol.* **2009**, *41*, 415; [61b] Y. Shiraishi, R. Miyamoto, T. Hirai, *J. Photochem. Photobiol. A: Chem.* **2008**, *200*, 432.